SHOCK-TUBE STUDY OF METHANE IGNITION WITH NO_2 AND N_2O

A Thesis

by

JOHN M. PEMELTON

Submitted to the Office of Graduate Studies of
Texas A&M University
in partial fulfillment of the requirements for the degree of

MASTER OF SCIENCE

August 2011

Major Subject: Mechanical Engineering

Shock-Tube Study of Methane Ignition with NO_2 and N_2O

SHOCK-TUBE STUDY OF METHANE IGNITION WITH NO_2 AND N_2O

A Thesis

by

JOHN M. PEMELTON

Submitted to the Office of Graduate Studies of
Texas A&M University
in partial fulfillment of the requirements for the degree of

MASTER OF SCIENCE

Approved by:

Chair of Committee,	Eric L. Petersen
Committee Members,	Kalyan Annamalai
	Rodney Bowersox
Head of Department,	Dennis O'Neal

August 2011

Major Subject: Mechanical Engineering

ABSTRACT

Shock-Tube Study of Methane Ignition with NO_2 and N_2O. (August 2011)

John M. Pemelton, B.S., Texas A&M University

Chair of Advisory Committee: Dr. Eric L. Petersen

NOx produced during combustion can persist in the exhaust gases of a gas turbine engine in quantities significant to induce regulatory concerns. There has been much research which has led to important insights into NOx chemistry. One method of NOx reduction is exhaust gas recirculation. In exhaust gas recirculation, a portion of the exhaust gases that exit are redirected to the inlet air stream that enters the combustion chamber, along with fuel. Due to the presence of NOx in the exhaust gases which are subsequently introduced into the burner, knowledge of the effects of NOx on combustion is advantageous. Contrary to general NOx research, little has been conducted to investigate the sensitizing effects of NO_2 and N_2O addition to methane/oxygen combustion.

Experiments were made with dilute and real fuel air mixtures of $CH_4/O_2/Ar$ with the addition of NO_2 and N_2O. The real fuel air concentrations were made with the addition of NO_2 only. The equivalence ratios of mixtures made were 0.5, 1 and 2. The experimental pressure range was 1 - 44 atm and the temperature range tested was 1177 – 2095 K. The additives NO_2 and N_2O were added in concentrations from 831 ppm to

3539 ppm. The results of the mixtures with NO_2 have a reduction in ignition delay time across the pressure ranges tested, and the mixtures with N_2O show a similar trend. At 1.3 atm, the NO_2 831 ppm mixture shows a 65% reduction and shows a 75% reduction at 30 atm. The NO_2 mixtures showed a higher decrease in ignition time than the N_2O mixtures. The real fuel air mixture also showed a reduction.

Sensitivity Analyses were performed. The two most dominant reactions in the NO_2 mixtures are the reaction $O+H_2 = O+OH$ and the reaction $CH_3+NO_2 = CH_3O+NO$. The presence of this second reaction is the means by which NO_2 decreases ignition delay time, which is indicated in the experimental results. The reaction produces CH_3O which is reactive and can participate in chain propagating reactions, speeding up ignition.

The two dominant reactions for the N_2O mixture are the reaction $O+H_2 = O+OH$ and, interestingly, the other dominant reaction is the reverse of the initiation reaction in the N_2O-mechanism: $O+N_2+M = N_2O+M$. The reverse of this reaction is the direct oxidation of nitrous oxide. The O produced in this reaction can then speed up ignition by partaking in propagation reactions, which was experimentally observed.

DEDICATION

To my family and friends. I would not be the same person without any of them.

ACKNOWLEDGEMENTS

I would like to thank my committee members Dr. Annamalai and Dr. Bowersox and especially my committee chair, Dr. Petersen for their support for this research.

I am also grateful to my friends, colleagues, and the incredible environment of Texas A&M University for making my time at here a great experience.

Lastly, thanks to my mother and father for all the countless ways they have supported me over the years.

TABLE OF CONTENTS

Page

LIST OF FIGURES

FIGURE Page

FIGURE Page

LIST OF TABLES

CHAPTER I

INTRODUCTION TO NOX CHEMISTRY AND LITERATURE REVIEW

Understanding NOx chemistry has practical applications due formation of NOx in the emissions of power producing engines. There has been research over the past few decades which led to important insights into NOx chemistry. The mechanisms that currently describe NOx production are the Zeldovich or Thermal NO, the Prompt NO, the N_2O mechanism, fuel nitrogen, and the newly added NNH mechanism.

The Zeldovich mechanism (Turns, 2000) was first proposed by Zeldovich in 1939 and consists of the following reactions:

(R1) $O+N_2 = NO+N$

(R2) $N+O_2 = NO+O$

(R3) $N+OH = NO+H$

This mechanism is primarily important in high-temperature combustion and is active in lean, rich, and stoichiometric mixtures. This mechanism is more significant at higher

---

This thesis follows the style of *Combustion Science and Technology*.

temperatures due to the energy required to break the N-N bond to make the atomic nitrogen produced in (R1).

The Prompt-NO or Fenimore mechanism was set forth by Fenimore in 1971 to describe the observation of NOx formation during the initial period of combustion (Fenimore, 1971). The Prompt-NO reactions are:

(R4) $CH+N_2 = HCN+N$

(R5) $C+N_2 = CN+N$

For mixtures with equivalence ratios that are less than 1.2, the Prompt-NO mechanism proceeds with the following reactions:

(R6) $HCN+O = NCO+H$

(R7) $NCO+H = NH+CO$

(R8) $NH+H = N+H_2$

(R9) $N+OH = NO+H$

For equivalence ratios greater than 1.2, the chemistry is more complicated and routes that inhibit NOx formation open up (Turns, 2000).

Barton and Dove (1969) and Malte and Pratt (1971) were among of the first to develop the N_2O mechanism. The N_2O mechanism is primarily responsible for producing NOx in low-temperature, lean combustion. The N_2O mechanism reactions are:

(R10) $O+N_2+M = N_2O+M$

(R11) $H+ N_2O = NO+NH$

(R12) $O+ N_2O = NO+NO$

Fuels that have nitrogen in the composition, such as coal, can oxidize to produce NOx (Turns, 2000). The mechanism that describes oxides of nitrogen that are formed from the combustion of fuels that contain nitrogen is called the fuel-nitrogen mechanism. The nitrogen in the fuel, during combustion, is converted to HCN or to NH_3. Afterwards, the NOx is made through the Prompt-NO mechanism. Figure 1 shows the reaction path that produces NOx from fuel nitrogen.

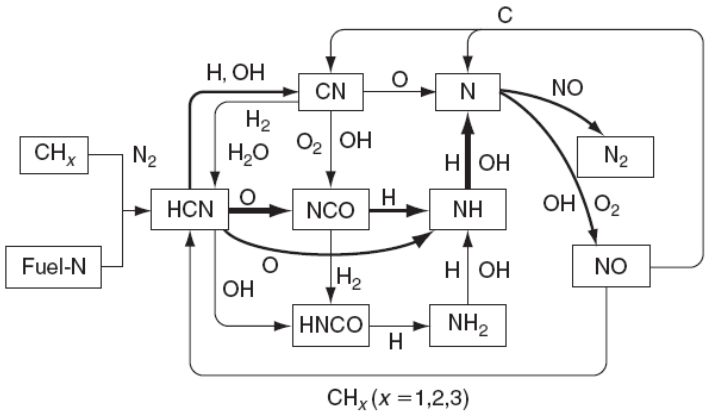

Figure 1. Fuel-nitrogen consumption route, via the Prompt-NO mechanism (Bowman et al., 1992).

The relatively new NNH mechanism, developed by Bozzelli and Dean (1995), produces NOx via the following two reactions:

(R13) $NNH = H+N_2$

(R14) $O+NNH = NH+NO$

The molecule NNH is first produced through the reverse of the fast reaction (R13), which is enhanced by quantum tunneling. Then, once NNH is in partial equilibrium via reaction (R1), the concentration of NNH is high enough to be involved in bimolecular reaction (R14) which directly produces NO.

Contrary to general NOx research, little has been conducted to investigate the sensitizing effects of NO_2 and N_2O addition to methane/oxygen combustion. One of the first works done in this area was conducted by Slack and Grillo (1981). They made mixtures of $CH_4/O_2/Ar$ with varying concentrations of NO_2 and conducted shock-tube experiments with the various mixtures that they made. They observed that the addition of NO_2 reduced ignition delay time. Slack and Grillo proposed that NO_2 is involved in an initiation step with methane and contributes to the decomposition of the methyl radical.

Slack and Grillo tested mixtures which contained methane, nitrogen dioxide, nitric oxide, argon, and oxygen. The baseline case was a half stoichiometric mixture of methane with an Ar diluency of 75%. The half stoichiometric methane mixtures were also made with 0.8% and 3.4% NO_2. The experimental results showed that both mixtures with NO_2 reduced ignition delay time; the 3.4% NO_2 mix reduced ignition delay time by an order of magnitude.

Mixtures which contained the additive NO were also tested. The small sensitizing effects that were noted were contributed to the NO to NO_2 conversion reaction: $NO+NO+O_2 = 2NO_2$. It was determined by Slack and Grillo that NO does not participate in reactions with methane or CH_4-O_2 generated radicals. This result does not agree with later investigations such by Sivaramakrishnan et al. (2007). In that work, it was shown that NO does partake in reactions that contributes to methane ignition.

To describe the experimental results obtained, Slack and Grillo proposed the following reactions take place:

(R15) $CH_4+NO_2 = CH_3+HNO_2$

(R16) $HNO_2+M = OH+NO+M$

(R17) $CH_4+OH = CH_3+H_2O$

(R18) $CH_3+NO_2 = CH_3O+NO$

(R19) $CH_3O+M = CH_2O+H+M$

(R20) $H+NO_2 = OH+NO$

Reactions (R15) through (R20) were used by Slack and Grillo to explain the experimental behavior that was observed during the various conditions that were tested.

Also tested were mixtures in which the relative concentration of one of the constituents was changed while maintaining the others constant. The mixtures tested which had no

oxygen still showed that NO_2 decayed. This result is important as it shows that NO_2 is primarily consumed in a reaction with methane. Reactions (R15) and (R16) are the initiation reactions through H-atom abstraction. Then reactions (R17) through (R20) demonstrate that oxygen is not required for NO_2 to fully decay. It was also observed that there was a direct conversion between NO and NO_2, or $-d\mathrm{NO_2}/d\mathrm{t} = d\mathrm{NO}/d\mathrm{t}$. The reactions (R18) and (R20) show this trend.

Argon concentration was shown by Slack and Grillo to play two roles in mixtures containing nitrogen dioxide, albeit contradictory ones. An increase in the total pressure of a given mixture (which was also an increase in argon concentration) would decrease ignition delay time, whereas an increase in the argon concentration relative to the other mixture constituents would decrease ignition delay time. The reaction (R19) demonstrates the ignition delay time sensitizing effects of an increase in total concentration. The cause of the contradictory desensitizing effects of an increase in argon concentration relative to the other mixture constituents was unknown to Slack and Grillo.

A more recent work by Gersen et al. (2010) also investigated the sensitizing effects of NO_2 on methane oxidation using a rapid compression machine. Gersen et al. and coworkers showed that methane/ethane mixtures are sensitized by NO_2, but the effect decreases with increasing pressure or decreasing temperature.

Gersen and coworkers made stoichiometric mixtures in real fuel air concentrations of methane, ethane, and a methane/ethane mixture. These mixtures were also made with

100-ppm and 270-ppm additions of NO_2. The results of comparing the methane mixture to the methane mixture doped with 270-ppm NO_2 indicate that nitrogen dioxide reduced ignition delay time, and that this reduction is temperature dependent. At a temperature of 1010 K, the 270-ppm mixture reduced ignition by more than a factor of 2, and at 910 K, it reduced it by only ~20%. The results were also compared on a time-versus-pressure graph, along an isotherm. Those results showed that nitrogen dioxide effects are also pressure dependent. A greater reduction of ignition delay time was noted at lower pressures than at higher pressures.

The ethane mixtures with and without 270-ppm NO_2 by contrast showed little difference in ignition delay time, and no temperature dependence was indicated. In the ignition delay time-versus-pressure results, there was also a slight decrease in ignition delay time for the 270-ppm mixture, but not a significant one, and no pressure dependence was shown. In general, for the temperatures and pressures tested, the 270-ppm NO_2 mixture decreased ignition time around 20-30%.

In the nature gas-simulating mixture of methane and ethane, ignition delay time was reduced compared to the pure methane mixture. The reduction in ignition delay time was also shown to be temperature dependent. At 900 K, the methane/ethane blend decreased ignition by ~50%, and at 1040 K, the decrease was a factor of 2. A mixture of methane/ethane doped with NO_2 was also made. The results for this mixture show that the NO_2-doped mixture reduces ignition time even further. A factor of 2 reduction was indicated at 1040 K, and a 30% decrease was observed at 900 K. Gersen et al. also

noted that the slopes of the ignition delay time-versus-inverse temperature plots were increased from the methane mixture when compared with the methane/ethane mixture and for the methane/ethane/270-ppm NO_2 mixture.

To explain the results that were observed, Gersen et al. proposed new consumption routes for CH_3 and for CH_3OO, that is:

(R21) $NO_2+CH_3 \rightarrow NO+CH_3OO$

(R22) $NO+CH_3OO \rightarrow NO_2+CH_3O$

Also of importance are the reactions that produce the chain-initiating radical OH through the NO/NO_2 conversion reactions:

(R23) $NO_2+H \rightarrow NO+OH$

(R24) $NO+HO_2 \rightarrow NO_2+OH$

Also, the direct initiation reaction of CH_4, as mentioned by Slack and Grillo, plays a significant role as well:

(R15) $CH_4+NO_2 = CH_3+HNO_2$

To elucidate the temperature and pressure dependence of the NO_2-doped mixtures, the analyses of Gersen et al. showed that formation of CH_3NO_2 play the dominant role:

(R25) $CH_3+NO_2(+M) = CH_3NO_2(+M)$

This reaction, which lowers the concentration of NO_2 available for other reactions, is active at lower temperatures and higher pressures, which agrees with the trends seen experimentally.

The effects of the NOx species NO_2 and N_2O on methane ignition can be used to calibrate a chemical kinetics mechanism containing NOx chemistry. The mechanism used in this study is a combination of the NO mechanism made by Sivaramakrishnan et al. (2007) and the C4 mechanism produced by Curran and coworkers (Healy et al., 2010).

Sivaramakrishnan et al. assembled a mechanism of 130 chemical species and 818 reversible chemical reactions that describe hydrocarbon-NOx chemistry. The model was based on a high-pressure natural gas blend mechanism developed by Sivaramakrishnan et al. and on hydrocarbon-NOx reactions produced at CNRS (Dagaut et al., 2006).

The flame chemistry, namely the H_2/O_2 reactions, in the model was updated by a model developed by Davis et al. (2005) which incorporates the results of recent studies that update thermodynamic parameters and reactions such as $H+O_2+M \rightarrow HO_2+M$ and $CO+OH \rightarrow CO_2+H$. Sivaramakrishnan et al. also replaced rate parameters for H_2/CO chemistry in the model with his findings (Sivaramkrishnan et al., 2007).

In reference (8), the two dominant NO-consuming, high-temperature reactions are:

(R26) $NO+OH \rightarrow NO_2+H$

(R27) $NO+HO_2 \rightarrow NO_2+OH$

The rate constant for (R26) was updated using recent shock-tube data produced by Srinivasan et al. (2007). Reaction (R27) was updated using the work of Ko and Fontijn (1991) who used flash photolysis/resonance fluorescence to obtain the results.

The key hydrocarbon-NOx reaction identified in the Sivaramakrishnan et al. reference (2007) was:

(R18) $CH_3+NO_2 = CH_3O+NO$

This reaction was also previously identified as significant by Slack and Grillo. The rate constant for this reaction was taken from the work of Yamada et al. (1981) which was obtained at room temperature and shows no temperature dependence.

The remaining, key NO-consuming reactions are those which include NO and CH_3O, C_2H_5O, CH_3O_2, and $C_2H_5O_2$. There were few studies that had the rate constant for these reactions at combustion temperatures. Consequently, Sivaramakrishnan et al. took the rate constants for these reactions from IUPAC evaluation for atmospheric chemistry (Atkinson et al., 1997). The thermochemical data for the hydrocarbon-NOx species in the model were taken from the online Burcat and Ruscic database (2005), and the ΔH_f^o data for CH_3NO_2 were taken from the model produced by Dagaut and coworkers (2005).

Sivaramakrishnan et al. ran experiments in a high-pressure shock tube and in a jet-stirred reactor. The high-pressure shock tube experiments were run at 46 and 49 atm, for temperatures between 1070 K and 1495 K. The mixtures utilized were lean natural gas blends both with and without 44 ppm of nitric oxide. In the jet-stirred reactor,

experiments were conducted at 10 atm and for temperatures of 800-1200 K. The jet-stirred mixtures were natural gas blends with ϕ=0.3-1.5, with both 0 and 200 ppm NO. In each of the experiments, the mole fraction of key species (CH_4, CO, H_2O, CH_2O, C_2H_4, C_2H_6, NO, NO_2, and HCN) was measured as a function of time. For the shock-tube experiments, the ignition delay time was also recorded.

The model developed in the Sivaramakrishnan et al. reference (2007) was compared to the experiments conducted. For the shock-tube jet-stirred reactor experiments without any NO added, the model had reasonable agreement with the mole fractions of the measured species. However, for the NO-doped mixture, the model demonstrated excellent agreement.

The C4 mechanism, used with the NO mechanism previously mentioned, has been under continuous developed for several years by Curran and coworkers (Healy et al., 2010) in collaboration with the present group at TAMU. The mechanism is based on the hierarchical characteristics of the combustion of hydrocarbons and contains H_2/O_2, CO/CH_4, C_2, C_3, and C_4 submechanisms that have been previously developed (Healy et al., 2010).

As discussed above, the production of NOx is important to engine manufacturers. One method of NOx reduction is exhaust gas recirculation. In exhaust gas recirculation as applied to a gas turbine, a portion of the exhaust gases that exits the turbine is redirected to the compressed-air stream that enters the combustion chamber, along with fuel (Cameretti et al., 2009). This rerouting is done so that the heat capacity of the mixture

entering the combustor is greater than it would be without the addition of the higher-energy exhaust gas, thereby lowering the temperature of the products of combustion. However, due to the presence of NOx in the exhaust gases, knowledge of the effects of NOx on combustion is advantageous. Figure 2 shows an exhaust gas recirculation scheme for a gas turbine.

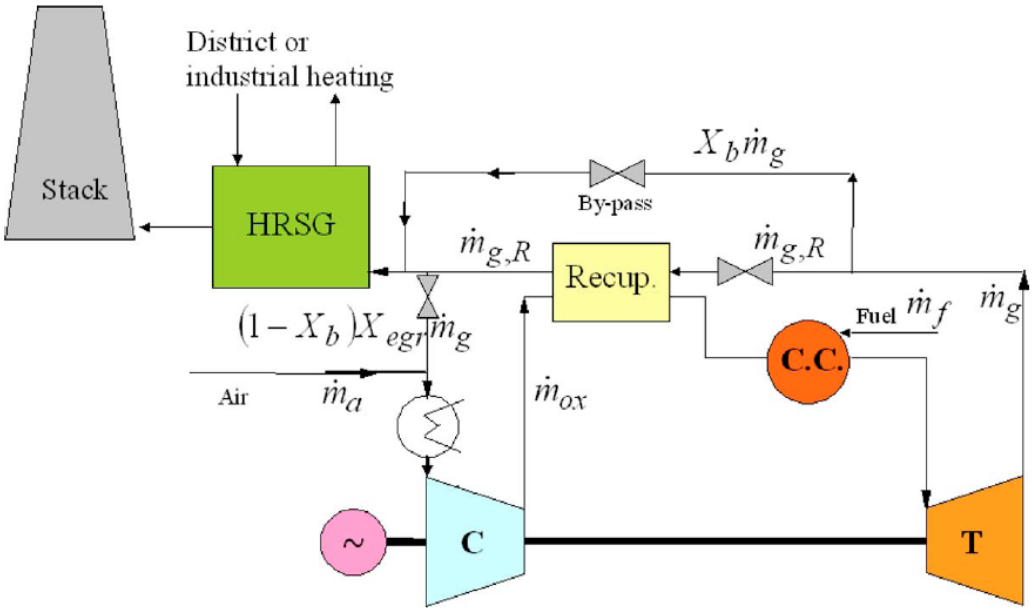

Figure 2. Exhaust gas recirculation schematic for a gas turbine engine (Cameretti et al., 2009).

The author has conducted experiments using a high-pressure shock-tube facility. Experiments were made with dilute mixtures of $CH_4/O_2/Ar$ with the addition of NO_2 and N_2O as well as mixtures of real fuel air concentrations with the addition of NO_2. Details on the experiments and the experimental procedure are provided in the next chapter.

The experiments were conducted at several pressures and temperature ranges appropriate for power generation gas turbines. The results are displayed by placing the log of the ignition delay time versus the inverse absolute temperature increased by a factor of 10000. The results are described in Chapter III. Lastly, Chapter IV contains the summary of the results obtain.

CHAPTER II

EXPERIMENTAL APPARATUS AND PROCEDURE

A high-pressure shock tube was employed to conduct the experiments of this study. The helium-driven shock tube is made with stainless steel 304. The length is 10.7 m and has an inner diameter of 16.2 cm, see Figure 3. A photomultiplier tube was utilized with a narrowband filter at 307 nm to record OH* chemiluminescence emission. The leading slope of the time history of the hydroxyl radical at an elevated state (OH*) was used for the determination of the ignition delay time for the experiments and for the model predictions (see Figure 4).

To determine the temperature and pressure behind the reflected shock wave, i.e. the temperature and pressure of the experiment, time-interval counters were used. The counters recorded the attenuation of the shock wave so that the shock speed is known at the endwall of the shock tube. Once the shock speed is known, the well-known Rankine-Hugoniot 1-D shock relations for a reflected shock wave can be used to calculate the temperature and pressure behind the reflected shock wave. For a typical experiment, the error in the calculated temperature is less than 1% (Petersen et al., 2005).

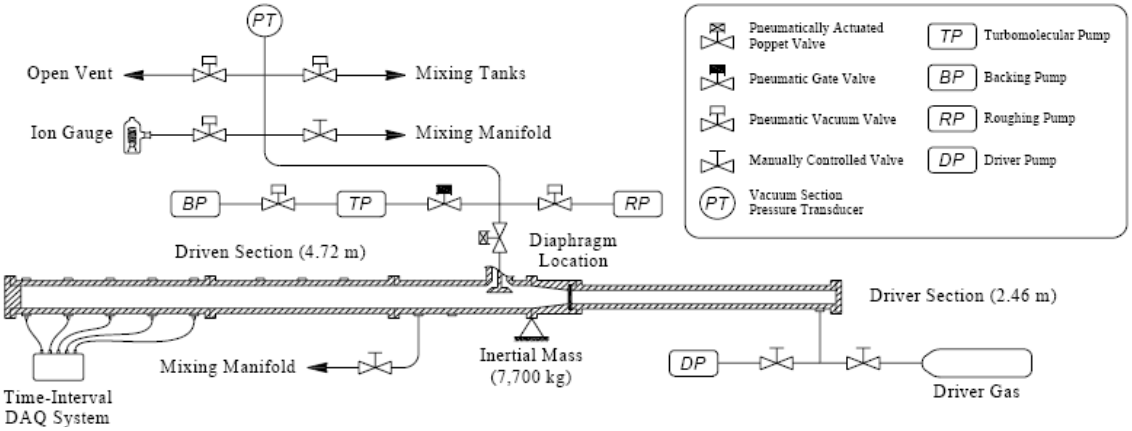

Figure 3. The high pressure shock tube as described by Aul et al. (2007).

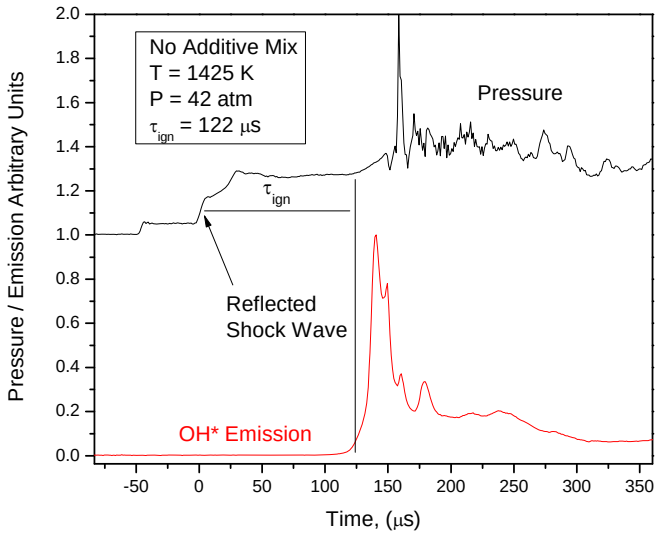

Figure 4. Determination of ignition delay time from OH* emission.

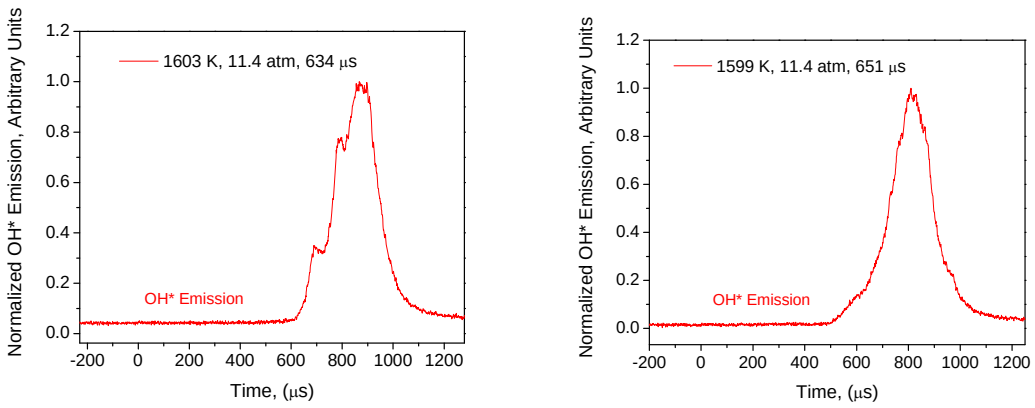

(a) (b)

Figure 5. Dilute mixtures of OH* emission (a) non-ideal trace and (b) ideal trace for nearly the same temperature.

In Fig. 5 is shown the results of OH* emission trace for the same mixture and at nearly the same temperature. It was noted that some of the experimental data obtained demonstrated the non-ideal trace of Fig. 5a. After running experiments at the same temperature and pressure for a given mixture, traces that show a more ideal behavior, such a Fig 5b were recorded. It was determine that the diluency percentage chosen for the dilute experiments, 97.5% Ar, is in the transition zone between real fuel air concentrations and ideally dilute concentrations. For mixtures with higher dilution concentrations such as 98% or 99% diluency, ideal traces are nominally expected and for real air fuel concentrations, more non-ideal behavior is recorded. Due to the present study's 97.5% diluency, both non-ideal and ideal behaviors were observed. However, the study's focus was in obtaining ignition delay time data, and the noted non-ideal characteristic does not bear on this recorded parameter.

CHAPTER III

RESULTS

DILUTE MIXTURE RESULTS

Several mixtures were studied during the test sequence, with a set of baseline mixtures with just methane and a set of mixtures with varying percentages of NOx additives. The dilute mixtures made were $CH_4/O_2/Ar$, ϕ = 0.5, 1, and 2 with 0%, 16.6% and 70.8% addition of NO_2 and N_2O. The experiments were conducted at pressures of about 1.3, 11, and 30 atm. The concentrations of each dilute mixture are indicated in Table 1. Nitrogen dioxide and nitrous oxide were added to the mixtures as a percent of the methane concentration (16.6% and 70.8%), and the Argon concentration was decreased in the amount equal to the NO_2 or N_2O addition.

Ignition delay times for the lower-pressure experiments with and without NO_2 are shown in Fig. 6. The 1.3-atm, 16.6% NO_2 mixture in Fig. 6 has a 65% reduction in ignition delay time compared to the 0% experiments, and the 70.8% mixture demonstrates an 80% reduction. For the 11-atm, 16.6% and 70.8% NO_2 mixtures, see Fig. 7, the results show a 60% and 90% reduction, respectively. In the 16.6% and 70.8% NO_2 30-atm mixtures, see Fig. 8, the data indicate a 75% and 91% reduction, respectively, in ignition delay time.

Similar results are seen for the experiments with N_2O addition; the 1.3-atm, 16.6% mixture demonstrates a trend of a 25% reduction, and the 70.8% mixture has a 60% reduction (Fig. 9). In the medium-pressure (11-atm) 16.6% and 70.8% N_2O mixtures (Fig. 10), the results show a 50% and 70% reduction, respectively. In the 30-atm, 16.6% and 70.8% N_2O mixtures, the ignition data show a 50% and 75% reduction, respectively (Fig. 11).

For the stoichiometric, low-pressure mixture (1.3-atm) with 16.6% NO_2 (Fig. 12) a 51% reduction was observed. In the medium-pressure (11-atm), 16.6% NO_2 mixture (Fig. 13) a 60% reduction in ignition delay time is indicated. The stoichiometric 16.6% N_2O mixture, 1.3 atm, in Fig 14, has a 31% decrease trend. The 11-atm counterpart in Figure 15 shows a 67% reduction.

Fuel-rich experiments, $\phi=2$, were also conducted. The 16.6% NO_2, 1.3-atm data shown in Fig. 16 demonstrate a 50% reduction in ignition delay time. The corresponding 11-atm data in Figure 17 indicate a 40% decrease. In Figure 18 are the $\phi=2$, 16.6% N_2O, 1.3-atm data. These data have a 50% reduction in ignition time. Finally, Fig. 19 contains the 16.6% N_2O, 11-atm data, and these data demonstrate a 50% decrease. In Figs. 6 through 19, the kinetics model when compared with the data demonstrates, in general, excellent agreement over all the conditions observed.

Table 1. Dilute mixture compositions.

Mix #	ϕ	CH_4 %	O_2 %	Ar %	NO_2 %	N_2O %
1	0.5	0.5	2	97.5	0	0
2	0.5	0.5	2	97.42	0.0831	0
3	0.5	0.5	2	97.15	0.3539	0
4	0.5	0.5	2	97.42	0	0.0831
5	0.5	0.5	2	97.15	0	0.3539
6	1	0.83	1.67	97.5	0	0
7	1	0.83	1.67	97.36	0.1383	0
8	1	0.83	1.67	97.36	0	0.1383
9	2	1.25	1.25	97.5	0	0
10	2	1.25	1.25	97.29	0.2081	0
11	2	1.25	1.25	97.29	0	0.2088

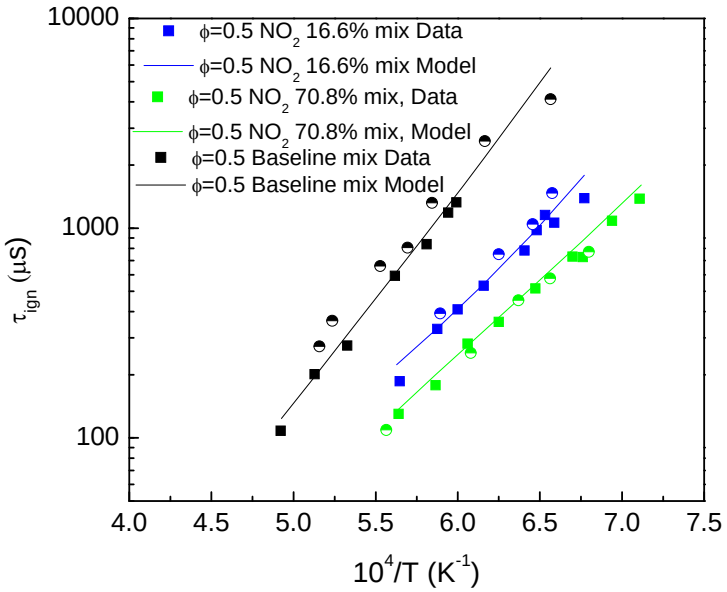

Figure 6. Ignition delay time results for the lean mixture at low pressure, 1.3 atm, for the ϕ =0.5 baseline, 16.6% and 70.8% mixes of NO_2.

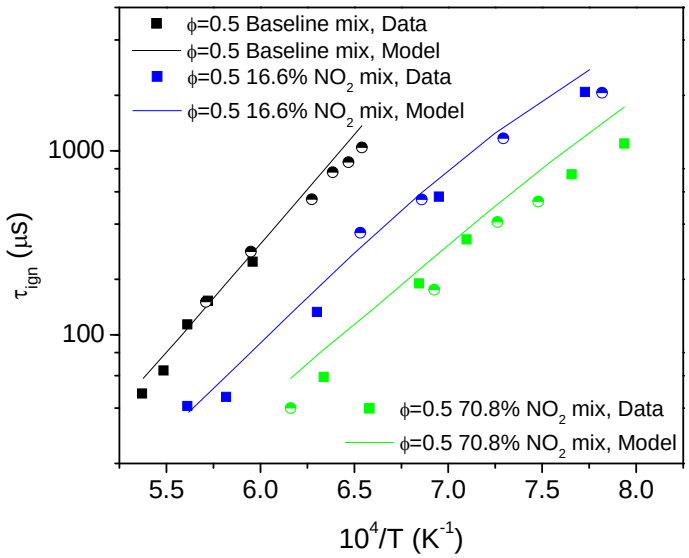

Figure 7. Ignition delay time results for the lean mixture at medium pressure, 11 atm, for the ϕ=0.5 baseline, 16.6% and 70.8% mixes of NO_2.

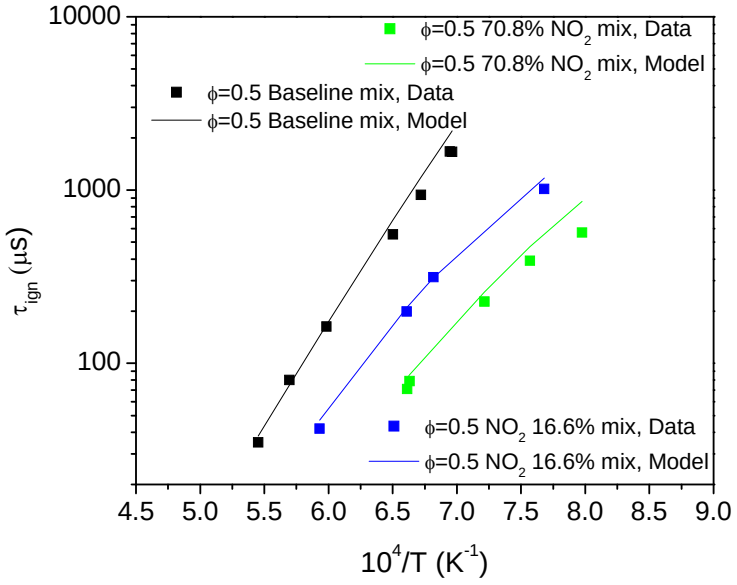

Figure 8. Ignition delay time results for the lean mixture at high pressure, 30 atm for the ϕ=0.5 baseline, 16.6% and 70.8% mixes of NO_2.

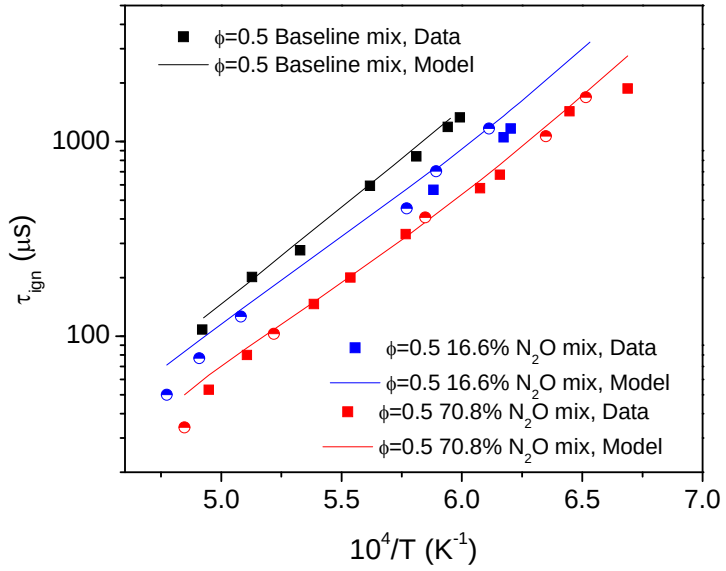

Figure 9. Ignition delay time results for the lean mixture at low pressure, 1.3 atm, for the ϕ=0.5 baseline, 16.6% and 70.8% mixes of N_2O.

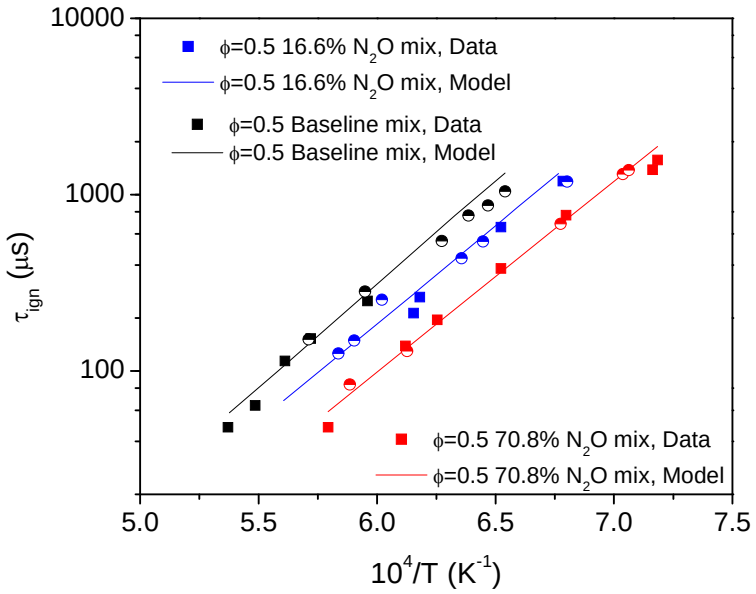

Figure 10. Ignition delay time results for the lean mixture at medium pressure, 11 atm, for the ϕ=0.5 baseline, 16.6% and 70.8% mixes of N_2O.

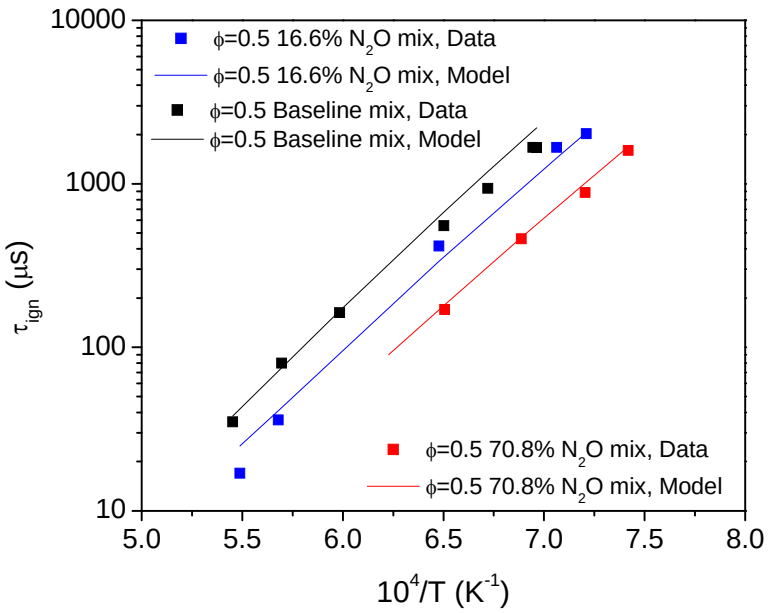

Figure 11. Ignition delay time results for the lean mixture at high pressure, 30 atm, for the ϕ=0.5 baseline, 16.6% and 70.8% mixes of N_2O.

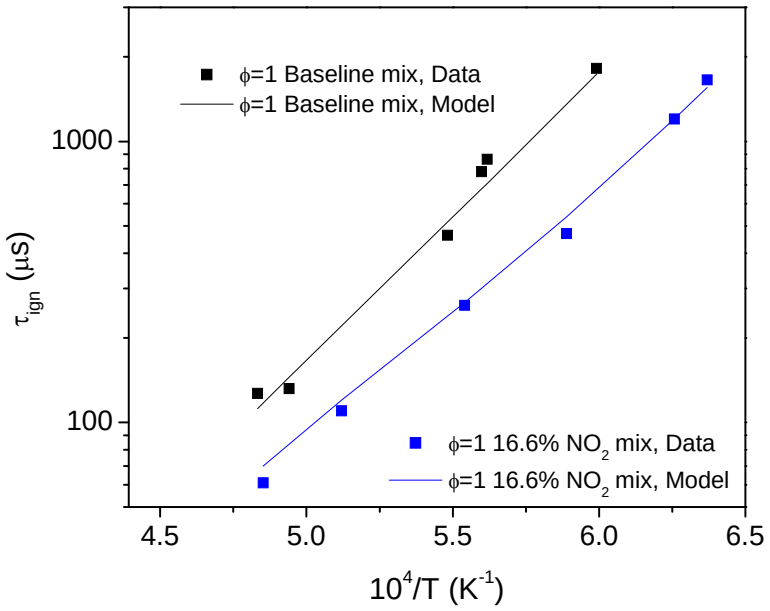

Figure 12. Ignition delay time results for the stoichiometric mixture at low pressure, 1.3 atm, for the ϕ=1 baseline and 16.6% mixes of NO_2.

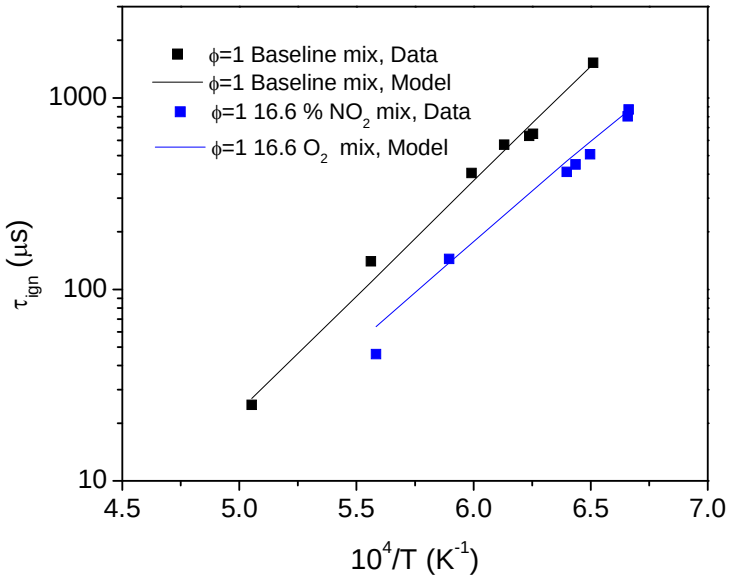

Figure 13. Ignition delay time results for the stoichiometric mixture at medium pressure, 11 atm, for the ϕ=1 baseline and 16.6% mixes of NO_2.

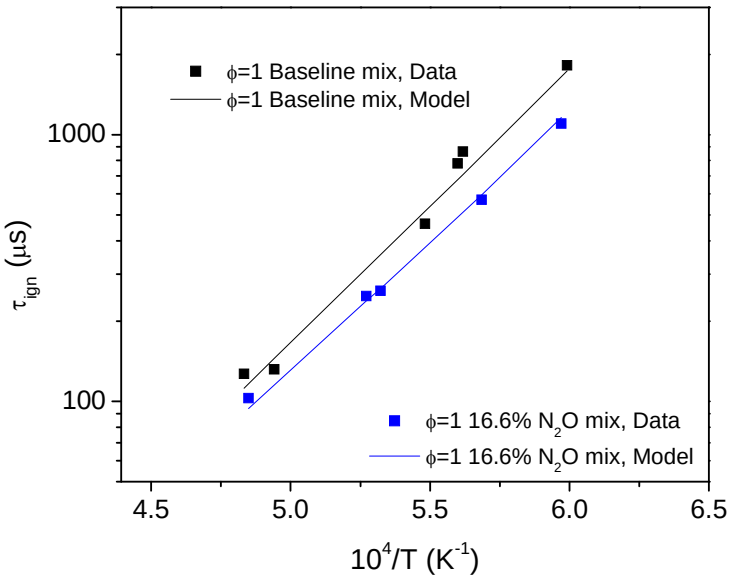

Figure 14. Ignition delay time results for the stoichiometric mixture at low pressure, 1 atm, for the ϕ=1 baseline, 16.6% mix of N_2O.

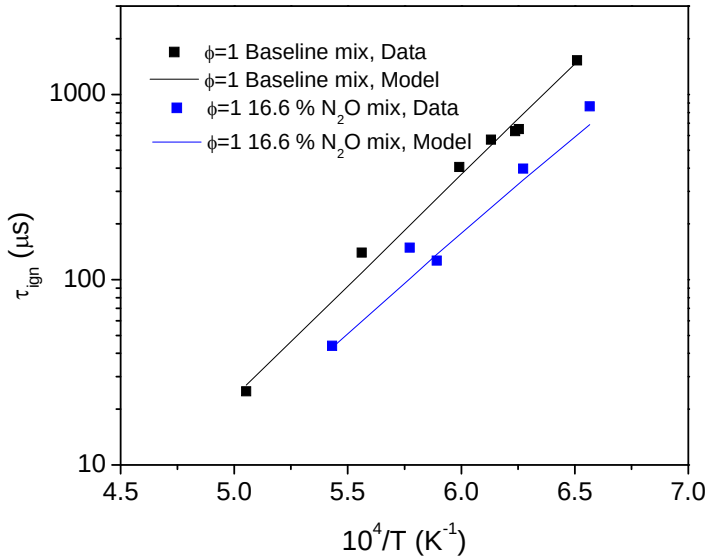

Figure 15. Ignition delay time results for the stoichiometric mixture at medium pressure, 11 atm, for the ϕ=1 baseline, 16.6% mix of N_2O.

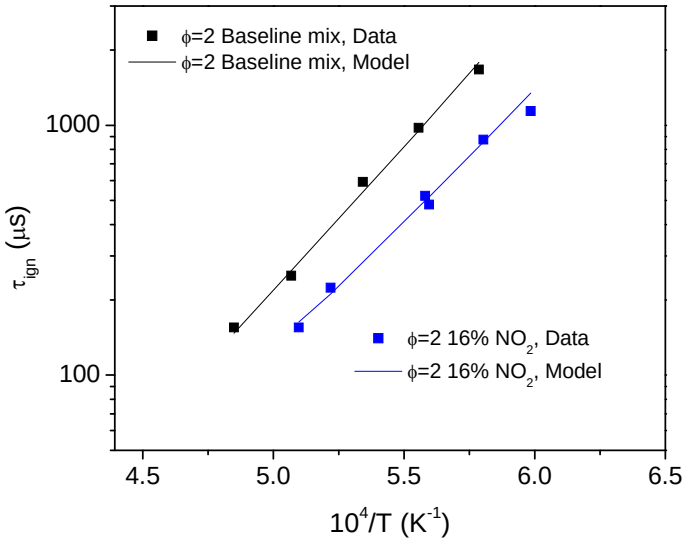

Figure 16. Ignition delay time results for the rich mixture at low pressure, 1 atm, for the ϕ=2 baseline, 16.6% mix of NO_2.

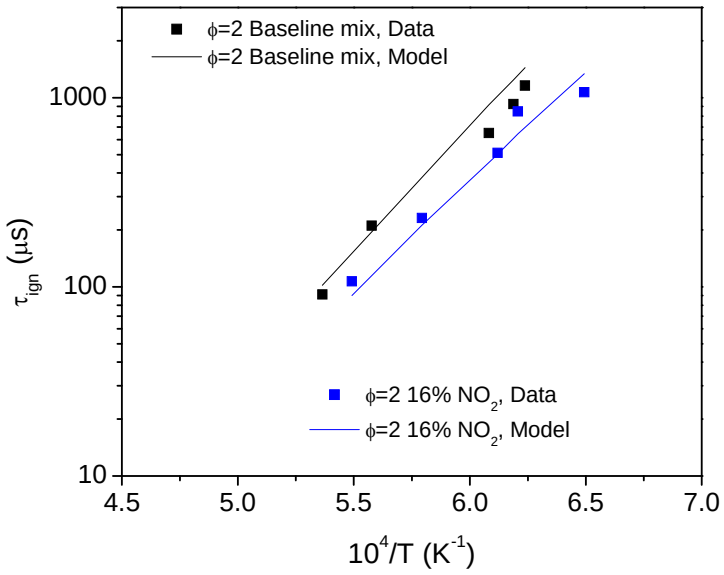

Figure 17. Ignition delay time results for the rich mixture at medium pressure, 11 atm, for the ϕ=2 baseline, 16.6% mix of NO_2.

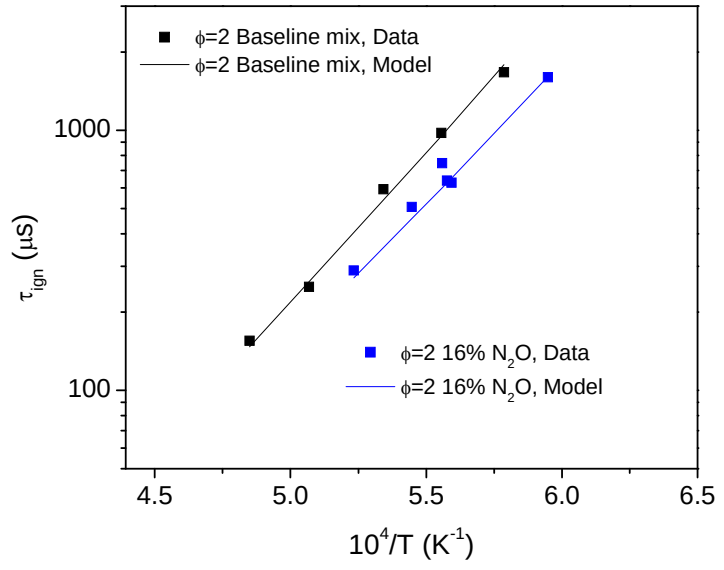

Figure 18. Ignition delay time results for the rich mixture at low pressure, 1 atm, for the ϕ=2 baseline, 16.6% mix of N_2O.

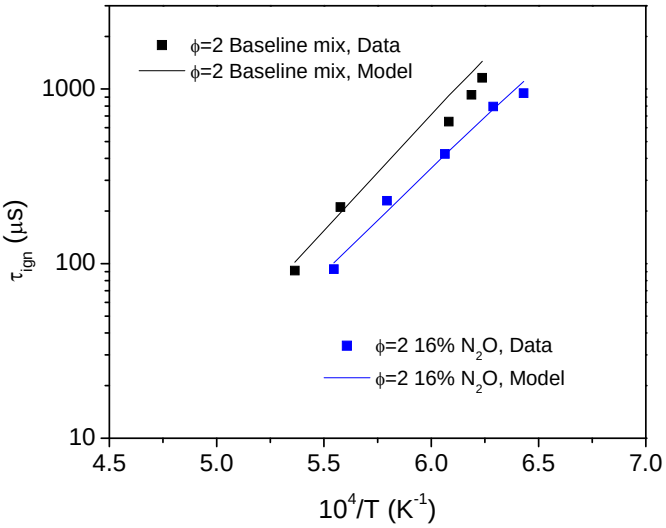

Figure 19. Ignition delay time results for the rich mixture at medium pressure, 11 atm, for the ϕ=2 baseline, 16.6% mix of N_2O.

REAL FUEL AIR RESULTS

The real fuel air mixtures made were $CH_4/O_2/N_2$ and Ar, with NO_2 as an additive. The equivalence ratios were ϕ = 0.5, 1, and 2. The scheme for the concentration of the additive is different than the dilute mixtures described above; mixtures with 0 ppm, and 1500 ppm addition of NO_2 were produced. Due to these species mixture concentrations varying significantly between the equivalence ratios tested, there were was not just one "intermediate pressure" amongst the experiments. The experiments were conducted at pressures of about 1.5, 9, 10, 14, and 44 atm. The concentrations of the mixtures are shown in Table 2.

Figures 20 – 22 contain the several pressure results for the mixtures which contain no additive. The trends indicate that ignition delay time is decreased with higher pressure and is reduced with increasing equivalence ratio.

The data for the lean mixture at 1.5 atm in Fig. 23 have a 60% reduction in ignition delay time. The 10-atm counterpart in Fig. 24 has a 67% decrease. The results in Figure 24 also show a slight temperature dependence of the 1500-ppm NO_2 data compared to the no-additive case. In the stoichiometric 1.5-atm results (Fig. 25), the trend has a 44% decrease. The corresponding 10-atm data in Figure 26 demonstrate a 44% reduction. Real fuel-air mixtures were also conducted for an equivalence ratio of 2. In Figure 27, the 2-atm data have a 47% decrease in ignition delay time. Lastly, the 9-atm rich mixture data, in Figure 28, have results for the effect of NO2 addition that are

temperature dependent. At 1500 K, there is no reduction, but at 1430 K there is a 40% decrease in ignition delay time.

The model used has good agreement with the data collected. For the fuel lean case, there is excellent agreement. The stoichiometric data show good agreement between data and model, but there is room for improvement in the model. Finally, the rich case has agreement between the model and data, but there is an even greater room for improvement than for the stoichiometric case.

Table 2. Real fuel air mixture compositions.

Mix #	ϕ	CH_4 %	O_2 %	N_2 %	Ar %	NO_2 %
12	0.5	5	20	75	0	0
13	0.5	5	20	60.25	14.67	0.1511
14	1	9.5	19	72	0	0
15	1	9.5	19	56.7	14.66	0.151
16	2	17	17	65	0	0
17	2	17	17	50	14.67	0.1512

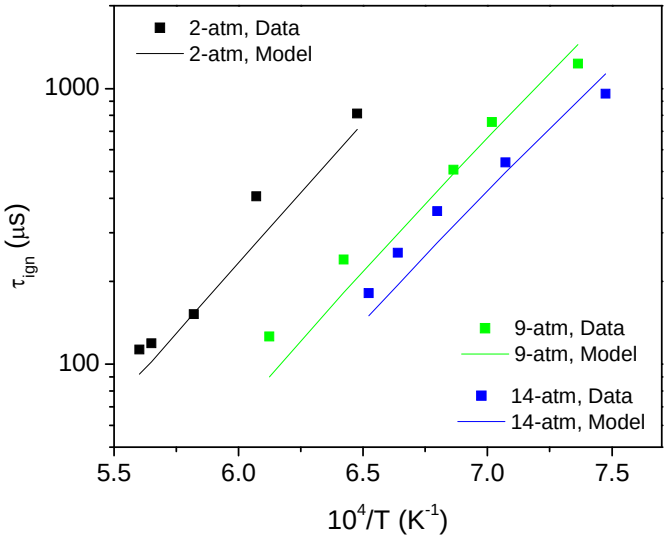

Figure 20. Ignition delay time results for the rich methane mixture at several pressures, ϕ=2 mixture.

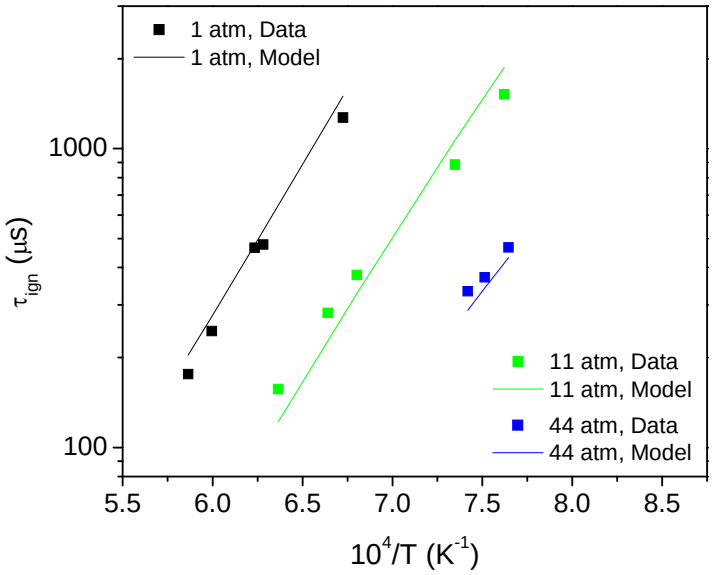

Figure 21. Ignition delay time results for the stoichiometric methane mixture at several pressures, ϕ=1 mixture.

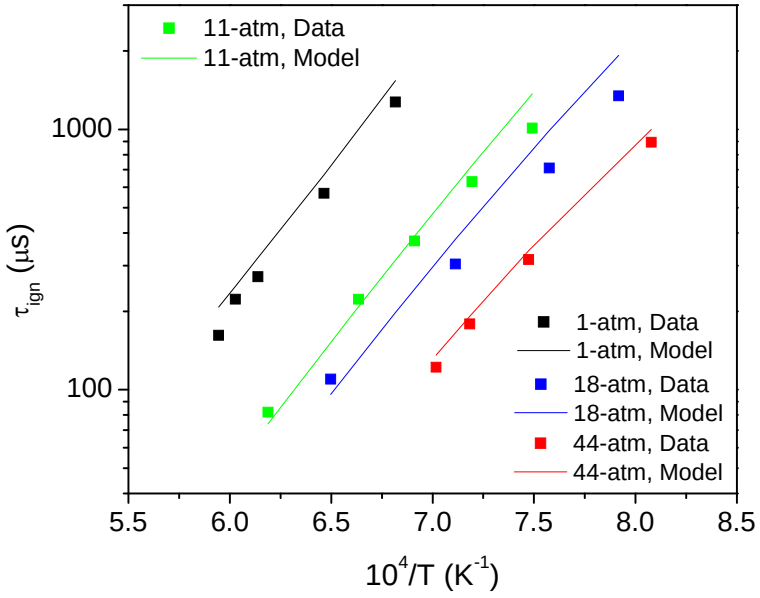

Figure 22. Ignition delay time results for the lean methane mixture at several pressures, ϕ=0.5 mixture.

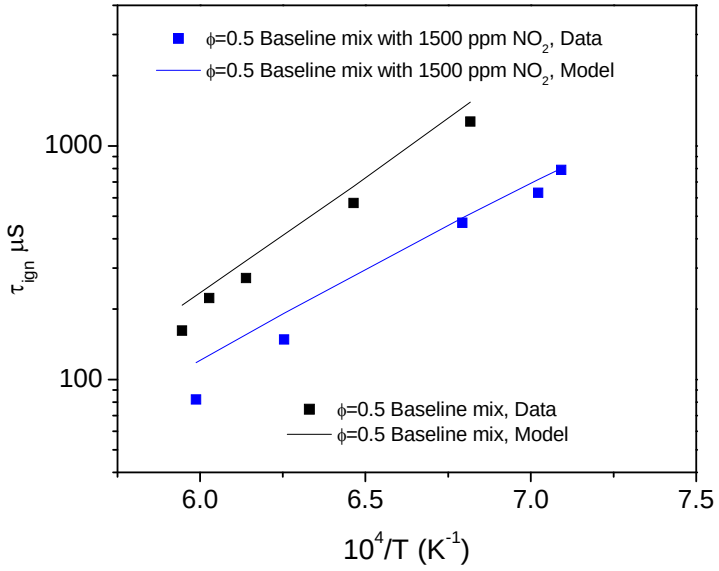

Figure 23. Ignition delay time results for the lean methane mixture at low pressure, 1.5 atm, ϕ=0.5 mixture, and the lean methane mixture with 1500 ppm NO_2.

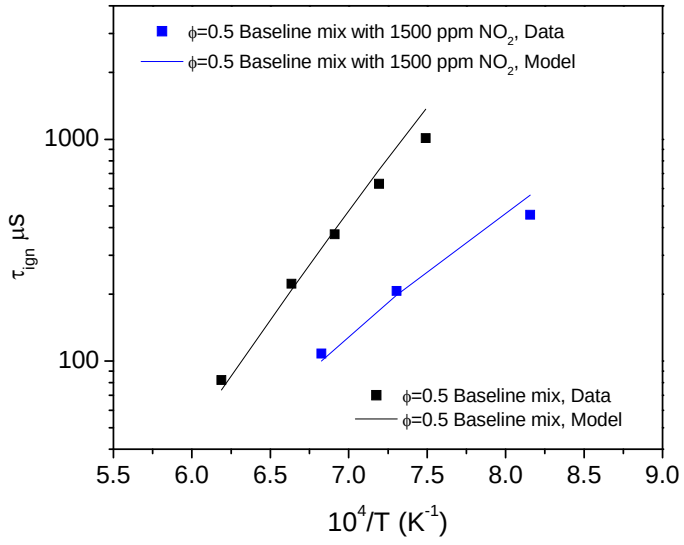

Figure 24. Ignition delay time results for the lean methane mixture at medium pressure, 10 atm, ϕ=0.5 mixture, and the lean methane mixture with 1500 ppm NO_2.

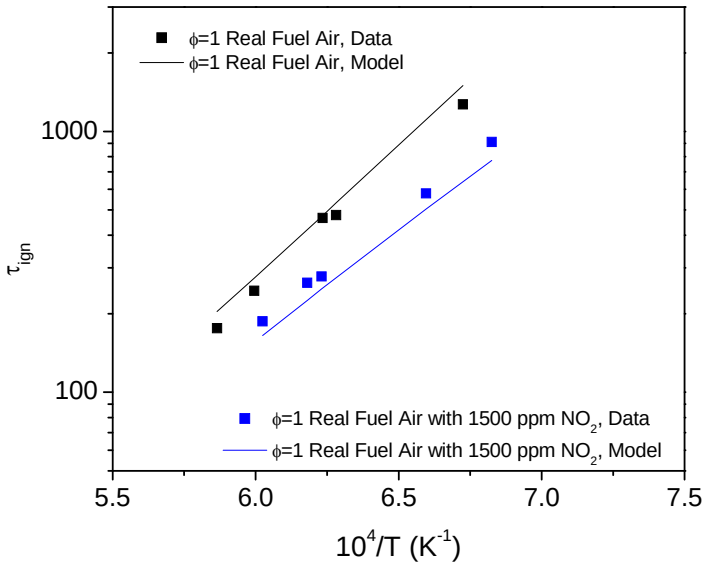

Figure 25. Ignition delay time results for the stoichiometric methane mixture at low pressure, 1.5 atm, ϕ=1 mixture, and the stoichiometric methane mixture with 1500 ppm NO_2.

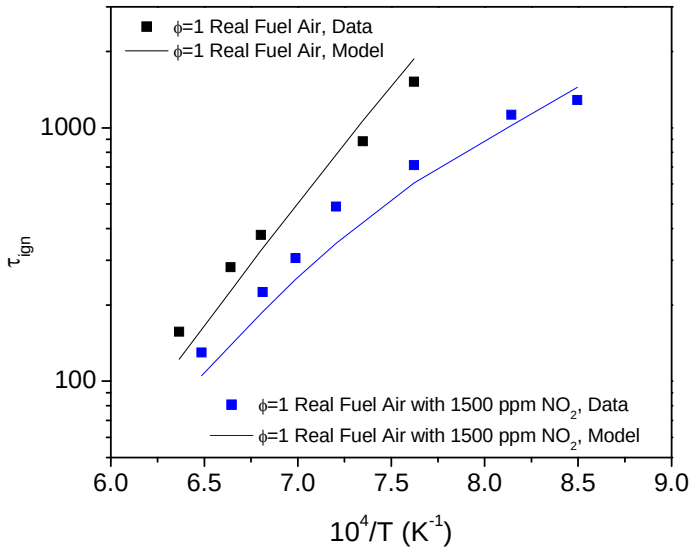

Figure 26. Ignition delay time results for the stoichiometric methane mixture at medium pressure, 10 atm, ϕ=1 mixture, and the stoichiometric methane mixture with 1500 ppm NO_2.

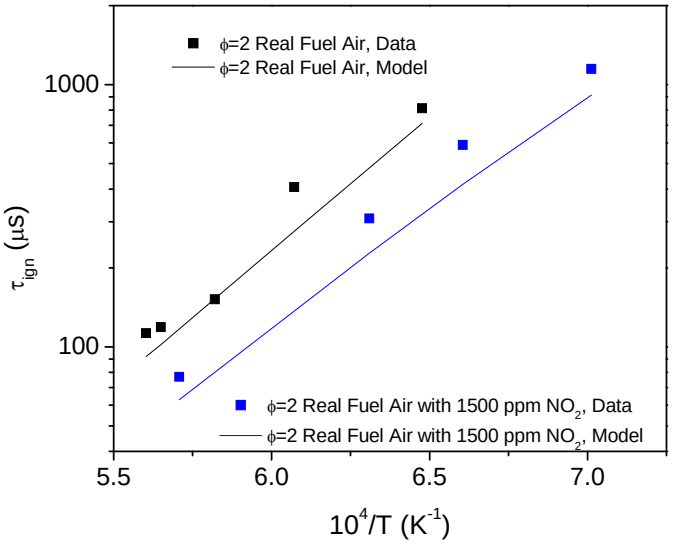

Figure 27. Ignition delay time results for the rich methane mixture at low pressure, 2 atm, ϕ=2 mixture, and the rich methane mixture with 1500 ppm NO_2.

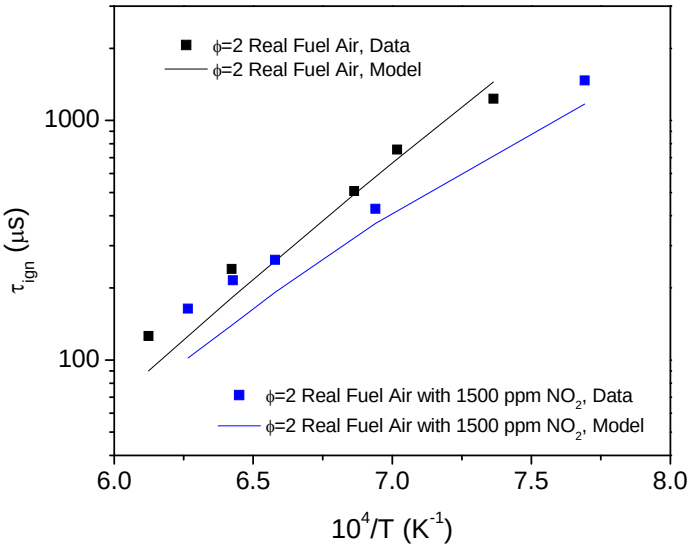

Figure 28. Ignition delay time results for the rich methane mixture at medium pressure, 9 atm, ϕ=2 mixture, and the rich methane mixture with 1500 ppm NO_2.

SENSITIVITY ANALYSIS RESULTS

The results for OH* sensitivity were obtained for several data points. The chemical kinetics sensitivity analysis is the partial derivative of the natural log of [OH*] with respect to the natural log of the reaction rate k of the i^{th} reaction in the mechanism used, i.e.:

$$\frac{\partial \ln[OH^*]}{\partial \ln(k_i)}$$

This partial derivative is then performed for all the reactions in the mechanism. Conducting this analysis is useful to indicate which reactions contribute to the concentration of OH*, either through adding or subtracting, at a particular instant in time during the experiment. Since OH* is used as the diagnostic for the experiments and also because it is present only at the time of the first signs of chemical reaction, an OH* sensitivity analysis also gives insight into the reactions that are important for ignition delay time. In this study the top 10 reactions are shown for the experiments analyzed.

Figure 29 shows the results for the dilute fuel lean mixture at 1733 and 1.3 atm. These conditions were chosen as representative of the lower-pressure experimental results for the dilute mixtures. The dominant two reactions for this experiment were:

(R28) $H+O_2 = O+OH$

(R29) $CH_3+H(+M) = CH_4(+M)$

Indeed, the reaction (R28) is the dominant reaction across all the sensitivity analyses obtained, in Figs. 29-34. This indicates that the production of the ignition diagnostic used, OH*, is most sensitive to reaction (R28), through difference in the mixtures made and the pressures run. Figures 30 and 31 are the OH* sensitivity results for the NO_2 and N_2O mixtures at atmospheric pressure. The two most dominant reactions in Fig. 30 are reaction (R28) and the following reaction:

(R18) $CH_3+NO_2 = CH_3O+NO$

This reaction was previously mentioned as a reaction proposed by Slack, which is involved in the oxidation of methane/nitrogen dioxide mixtures. Reaction (R18) was also identified by Sivaramakrishnan as the key hydrocarbon-NOx reaction. The presence of reaction (R18) in the results of Figure 30 shows the means by which NO_2 decreases ignition delay time, as indicated in the experimental results. Reaction (R18) produces CH_3O which is much more reactive than the methyl radical and can participate in chain propagating reactions, thus speeding up ignition.

In the Fig. 31, the two dominant reactions for the atmospheric N_2O mixture are the reaction (R28) and, interesting to note, the other dominant reaction is the reverse of the initiation reaction in the N_2O-mechanism:

(R10) $O+N_2+M = N_2O+M$

The reverse of this reaction is the decomposition of nitrous oxide, which produces atomic oxygen. The O produced in this reaction can then speed up ignition by partaking in propagation reactions, which was experimentally observed.

Figures 32 through 34 demonstrate the same mixtures as Figs. 29 – 31 but at approximately 11 atm. The dominant reactions in the results are the same as their atmospheric counterparts. The remaining 8 reactions are approximately the same as the reactions found in the 1-atm case, indicating that these reactions are common to both the CH_4/NO_2 and CH_4/N_2O experiments.

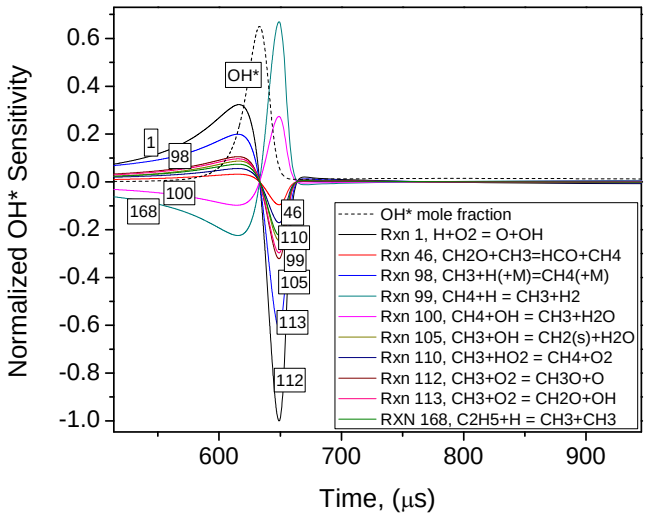

Figure 29. Normalized OH* Sensitivity for Mix 1, 1780 K, 1.3 atm.

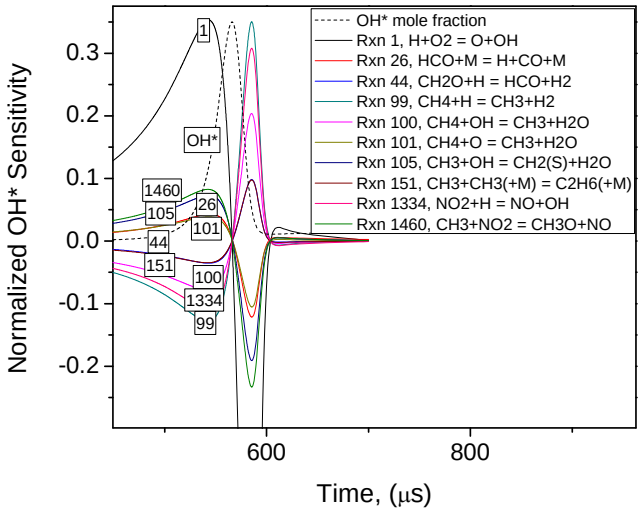

Figure 30. Normalized OH* Sensitivity for Mix 2, 1624 K, 1.4 atm.

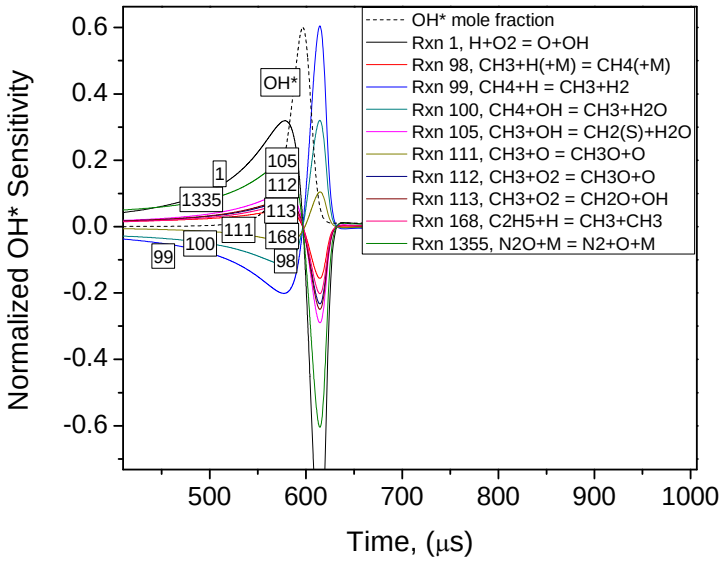

Figure 31. Normalized OH* Sensitivity for Mix 4, 1733 K, 1.3 atm.

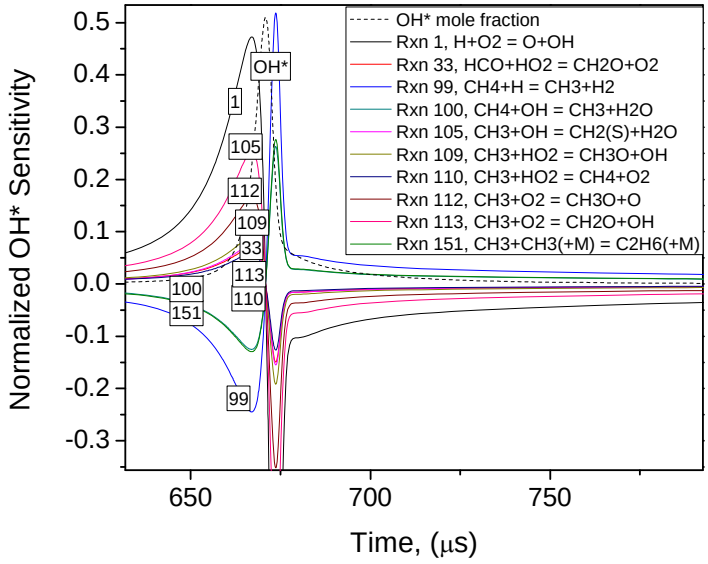

Figure 32. Normalized OH* Sensitivity for Mix 1, 1594 K, 10.5 atm.

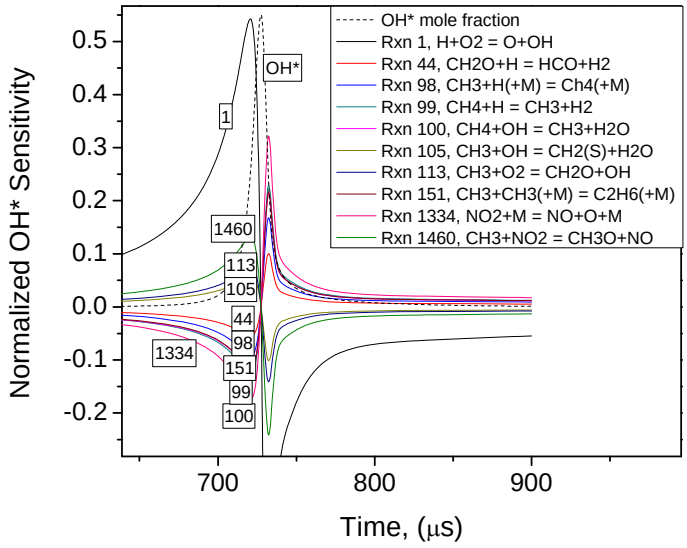

Figure 33. Normalized OH* Sensitivity for Mix 2, 1439 K, 11.5 atm.

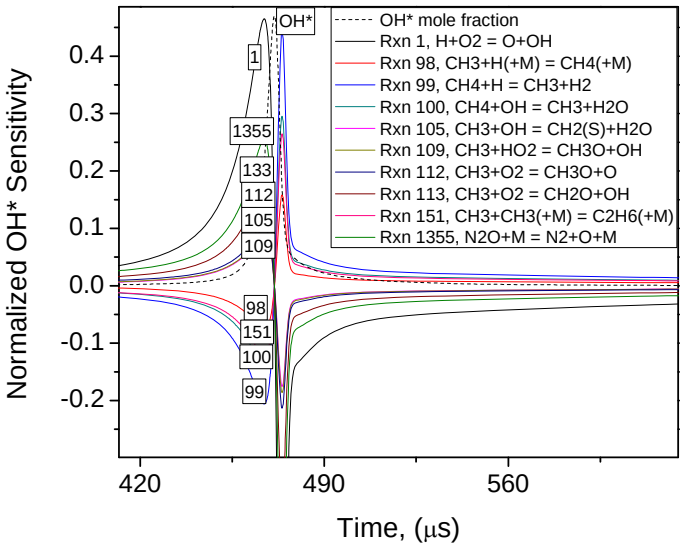

Figure 34. Normalized OH* Sensitivity for Mix 4, 1573 K, 11.3 atm.

CHAPTER IV

SUMMARY AND CONCLUSION

The formation of oxides of nitrogen, NOx chemistry, is important due to emissions regulations. Research has been conducted to better understand the formation of oxides of nitrogen during combustion. This community-wide effort has led to the development of the NOx mechanisms. The mechanisms that currently describe NOx production are the Zeldovich or Themal NO, the Prompt NO, the N_2O mechanism, fuel nitrogen, and the newly added NNH mechanism.

Dilute mixtures were made with methane/oxygen/argon and varying concentrations of nitrogen dioxide and nitrous oxide, similar to the work of Slack and Grillo, to assess the nitrogen oxide chemistry within a larger mechanism that has been validated for methane oxidation. Data were obtained over a wide range of temperatures and pressures in a high-pressure shock-tube facility. Various mechanisms have been developed to describe the formation of the NOx. The kinetics model used in this study is a combination of an NO-mechanism produced by Sivaramakrishnan et al., and a C4 mechansim developed by Curran and coworkers.

The dilute mixtures made with an addition of NO_2 in general demonstrate a greater reduction in ignition delay compared to the mixtures made with an addition of N_2O. The results of the mixtures with NO_2 have a similar reduction in ignition delay time across the pressure ranges tested, and the mixtures with N_2O show a similar trend. The model

shows a very good to excellent agreement with the data across the temperatures, pressures and mixtures studied.

Real fuel-air mixtures were also made with methane/oxygen/argon and a constant concentration of nitrogen dioxide of 1500 ppm. The mixtures were for equivalence ratios of 0.5, 1, and 2. Like the dilute mixtures, there was a reduction in ignition delay time. It was noted that as the equivalence ratio increased, the ignition delay time was not reduced by the same amount as lower ratios.

Sensitivity analyses were also performed. The two most dominant reactions in the NO_2 mixtures are reaction (R28)

(R28) $H+O_2 = O+OH$

and the following reaction:

(R18) $CH_3+NO_2 = CH_3O+NO$

This reaction was previously mentioned as a reaction proposed by Slack and Grillo, which is involved in the oxidation of methane/nitrogen dioxide mixtures. This reaction was also identified by Sivaramakrishnan et al. as the key hydrocarbon-NOx reaction. Reaction (R18) produces CH_3O which is reactive and can participate in chain propagating reactions, speeding up ignition, which was observed experimentally.

The two dominant reactions for the N_2O mixture are the reaction (R28) and, interesting to note, the other dominant reaction is the reverse of the N_2O formation reaction in the N_2O-mechanism:

(R10) $O+N_2+M = N_2O+M$

The reverse of this reaction is the decomposition of nitrous oxide, which produces the atomic oxygen. The O produced in this reaction can then speed up ignition by partaking in propagation reactions, which was experimentally observed.

REFERENCES

Atkinson, R., Baulch, DL., Cox, RA., Hampson, RF., Kerr, JA., Rossi, MJ., Troe, J. 1997. Evaluated Kinetic, Photochemical and Heterogeneous Data for Atmospheric Chemistry: Supplement V. IUPAC Subcommittee on Gas Kinetic Data Evaluation for Atmospheric Chemistry. *J. Phys. Chem. Ref. Data*, **26**, 521-1011.

Aul, CJ., de Vries, J., Petersen, EL. 2007. New Shock-Tube Facility for Studies in Chemical Kinetics at Engine Conditions. Eastern States Fall Technical Meeting of the Combustion Institute, Oct 21-21, Charlottesville, VA.

Barton, SC., Dove, JE. 1969. Mass Spectroscopic Studies of Chemical Reactions in Shock Waves: The Thermal Decomposition of Nitrous Oxide. *Canadian J. Chem*., **47,** 521.

Bowman, CT. 1992. Control of Combustion-Generating Nitrogen Oxide Emissions: Technology Driven by Regulations. *Sym. Combust*., **24**, 859-878.

Bozzelli, JW., Dean, AM. 1995. O+NNH: A Possible New Route for NOx Formation in Flames. *Int. J Chem. Kint,.* **27**, 1097-1109.

Burcat, A., Ruscic, B. 2005. Thrid Millennium Ideal Gas and Condensed Phase Thermochemical Database for Combustion with Updates from Active Thermochemical Tables. Report ANL 05-20 and TAE 960. Electronic format: ftp://ftp.technion.ac.il/pub/supported/aetdd/thermodynamics/

Cameretti, MC., Piazzesi, R., Reale, F., Tuccillo, R. 2009. Combustion Simulation of an Exhaust Gas Recirculation Operated Micro-Gas Turbine. *J. Eng. Gas Turb. Power*, **131,** 051701-1 - 051701-10.

Dagaut, P., Dayma, G. 2006. Mutual Sensitization of the Oxidation of Nitric Oxide and a Natural Gas Blend in a JSR at Elevated Pressure: Experimental and Detailed Kinetic Modeling Study. *J. Phys. Chem. A,* **110**, 6608-6616.

Dagaut, P., Nicolle, A. 2005. Experimental Study and Detailed Kinetic Modeling of the Effect of Exhaust Gas on Fuel Combustion: Mutual Sensitization of the Oxidation of Nitric Oxide and Methane over Extended Temperature and Pressure Ranges. *Combust. Flame*, **140**, 161-171.

Davis, SG., Joshi, A., Wang, H., Egolfopoulos, F. 2005. An Optimized Kinetic Model of H_2/CO Combustion . *Proc. Combust. Inst*., **30**, 1283-1292.

Fenimore, CP. 1971. Formation of Nitric Oxide in Premixed Hydrocarbon Flames. *Proc. Combust. Inst.*, **13,** 373-380.

Gersen, S., Mokhov, AV., Darmeveil, JH., Levinsky, HB., Glarborg, P. 2011. Ignition-Promoting Effect of NO_2 on Methane, Ethane and Methane/Ethane Mixtures in a Rapid Compression Machine. *Proc. Combust. Inst*, **33**, 433-440.

Healy, D., Kopp, MM., Polley, NL., Petersen, EL., Bourque, G., Curran, HJ. 2010. Methane/n-Butane Ignition Delay Measurements at High Pressure and Detailed Chemical Kinetics Simulations. *Energy Fuels,* **24**, 1617-1627.

Ko, T., Fontijn, A. 1991. High-Temperature Photochemistry Kinetics Study of the Reaction $H + NO_2 \rightarrow OH + NO$ from 296 to 760 K. *J. Phys. Chem.*, **95**, 3984-3987.

Malte, PC., Pratt, DT. 1971. The Role of Energy-Releasing Kinetics in NOx Formation: Fuel-Lean, Jet Stirred CO-Air Combustion. *Combust. Sci. Tech.,* **9**, 221-231.

Petersen, EL., Richard, MJA., Crofton, MW., Abbey, ED., Traum, MJ., Kalitan, DM. 2005. A Facility for Gas- and Condensed-Phase Measurements behind Shock Waves. *Meas. Sci. Technol.* **16,** 1716-1729.

Sivaramakrishnan, R., Brezinsky, K., Dayma, G., Dagaut, P. 2007. High Pressure Effects on the Mutual Sensitization of the Oxidation of NO and CH_4-C_2H_6 Blends. *Phy. Chem. Chemical Phyics,* **9**, 4230-4244.

Slack, MW., Grillo, AR. 1981. Shock Tube Investigation of Methane-Oxygen Ignition Sensitized by NO_2. *Combustion and Flame,* **40**, 155-172.

Srinivasan, NK., Su, M.-C., Sutherland, JW., Michael, JV., Ruscic, B. 2007. Reflected Shock Tube Studies of High-Temperature Rate Constants for $OH + NO_2 \rightarrow HO_2 + NO$ and $OH + HO_2 \rightarrow H_2O + O_2$. *J. Phys. Chem. A,* **105**, 6602-6607.

Turns, SR. 2000. *An Introduction to Combustion*. McGraw Hill, Boston, Massachusetts.

Yamada, F., Slagle, IR., Gutman, D. 1981. Kinetics of the Reaction of Methyl Radicals with Nitrogen Dioxide . *Chem. Phys. Lett.*, **83**, 409-412.

APPENDIX A

Table 3. Shock-tube experimental data.

Mix #	T (K)	P (atm)	P_{avg}	τ_{ign} (μs)	Mix #	T (K)	P (atm)	P_{avg}	τ_{ign} (μs)
1	2032	1.23	1.3	108	2	1782	11.17	11.5	41
	1950	1.27		201		1719	11.04		46
	1877	1.31		276		1439	11.61		564
	1780	1.32		593		1294	12.18		2089
	1721	1.34		839		1587	11.51		133
	1669	1.37		1329	2	1600	0.95	0.95	950
	1683	1.34		1187		1521	0.96		1858
1	1862	10.67	10.7	48		1697	0.95		404
	1782	10.46		114		1549	0.95		1321
	1823	10.69		64	2	1371	11.97	11.4	1166
	1748	10.84		153		1279	11.26		2063
	1678	10.68		250		1458	11.25		544
1	1523	0.88	0.94	5210		1531	10.91		359
	1939	0.93		346	2	1467	26.48	26.9	314
	1910	0.92		458		1513	25.75		199
	1622	0.97		3289		1686	25.72		42
	1711	0.96		1669		1302	29.57		1013
	1756	0.95		1021	3	1650	1.37	1.4	281
	1809	0.94		834		1705	1.34		178
1	1566	10.8	10.5	763		1773	1.32		130
	1546	10.33		868		1600	1.39		358
	1529	9.92		1044		1545	1.39		516
	1594	10.65		546		1493	1.4		733
	1681	10.5		283		1479	1.41		727
	1751	10.64		151		1441	1.43		1085
1	1834	25.59	26	35		1407	1.41		1383
	1756	25.91		80	3	1578	11.23	11.7	59
	1671	25.81		163		1461	11.24		190
	1538	25.94		555		1409	11.65		330
	1440	26.27		1670		1260	12.20		1096
	1436	26.51		1665		1306	12.13		744
	1488	26.06		939	3	1645	1.37	1.4	254
2	1771	1.30	1.4	186		1797	1.31		109
	1702	1.32		331		1570	1.37		453
	1667	1.37		410		1524	1.39		576
	1624	1.40		531		1471	1.39		772
	1477	1.38		1389	3	1623	11.31	11.8	40
	1518	1.40		1064		1444	11.28		176
	1561	1.39		782		1377	12.17		410
	1543	1.40		977		1337	12.24		529
	1531	1.42		1154					

Mix #	T (K)	P (atm)	P_{avg}	τ_{ign} (μs)	Mix #	T (K)	P (atm)	P_{avg}	τ_{ign} (μs)
3	1508	28.21	29.4	79	5	2063	1.27	1.3	34
	1512	27.39		71		1916	1.25		103
	1386	29.75		227		1710	1.3		408
	1321	30.69		391		1575	1.37		1066
	1254	31.1		569		1535	1.4		1688
4	1620	1.39	1.4	1051	5	1476	11.44	11.5	683
	1612	1.33		1167		1632	11.16		130
	1700	1.35		565		1699	11.38		84
4	1625	11.5	11.7	213		1421	11.5		1309
	1533	11.72		655		1416	11.8		1380
	1474	11.76		1192	5	1537	27.83	28.6	170
	1618	11.82		262		1348	29.33		1597
4	2037	1.24	1.3	77		1388	29.1		885
	2095	1.22		50		1452	28.03		461
	1968	1.29		126	6	1669	1.4	1.3	1818
	1733	1.32		453		2024	1.22		132
	1636	1.38		1166		2069	1.22		127
	1697	1.37		704		1824	1.23		464
4	1470	11.35	11.3	1186		1780	1.34		864
	1551	11.51		544		1786	1.35		780
	1573	11.32		437	6	1669	11.28	11.3	406
	1694	11.26		149		1979	10.89		25
	1713	11.19		126		1798	11.01		140
	1661	11.36		254		1631	11.75		571
4	1822	26.22	28.1	17		1603	11.44		634
	1761	26.86		36		1599	11.4		651
	1544	28.41		417		1536	11.51		1526
	1416	29.36		1671	7	1953	1.31	1.4	110
	1387	29.79		2022		2061	1.29		61
5	1734	1.4	1.4	335		1805	1.33		261
	1806	1.37		200		1698	1.45		470
	1857	1.31		146		1598	1.46		1201
	2021	1.23		53		1570	1.42		1654
	1495	1.42		1872	7	1696	10.7	11.3	144
	1551	1.42		1431		1791	10.54		46
	1624	1.44		676		1563	11.12		411
	1646	1.37		575		1554	11		450
	1958	1.3		80		1539	11.67		508
5	1726	11.36	11.7	48		1502	12.02		801
	1634	11.77		139		1501	12		872
	1533	11.88		382	8	1879	1.39	1.3	260
	1471	11.88		766		2062	1.27		103
	1392	12.01		1570		1675	1.4		1100
	1396	11.34		1383		1759	1.36		570
	1599	11.81		195		1897	1.29		248

Mix #	T (K)	P (atm)	P_{avg}	τ_{ign} (μs)	Mix #	T (K)	P (atm)	P_{avg}	τ_{ign} (μs)
8	1732	10.84	11.4	149	12	1263	21.3	18.4	1345
	1841	10.77		44		1320	19.27		711
	1697	11.44		127		1406	17.32		304
	1523	12.05		862		1539	15.79		110
	1594	12.11		398	12	1238	48.22	44	894
9	1800	1.34	1.3	976		1392	42.62		179
	1973	1.23		250		1338	42.96		316
	2062	1.23		155		1425	42.01		122
	1872	1.29		593	13	1670	1.63	1.8	82
	1728	1.34		1669		1599	1.71		148
9	1644	11.16	11	650		1472	1.81		469
	1793	10.59		211		1424	1.86		630
	1864	10.62		91		1410	1.99		789
	1616	11.24		925	13	1465	12.92	12.9	108
	1603	11.54		1159		1369	13.52		207
10	1787	1.31	1.3	481		1226	12.16		457
	1916	1.28		224	14	1487	1.55	1.4	1270
	1962	1.26		155		1668	1.29		245
	1792	1.37		522		1705	1.21		176
	1723	1.39		875		1592	1.42		478
	1671	1.35		1140		1604	1.36		466
10	1726	10.97	11.1	231	14	1312	12.26	10.5	1519
	1821	10.79		107		1470	10.2		378
	1634	10.96		511		1571	9.26		157
	1611	11.55		847		1361	11.36		884
	1540	11.2		1071		1506	9.58		282
11	1799	1.33	1.3	747	14	1331	42.51	42.7	371
	1836	1.26		507		1308	44.19		467
	1911	1.28		289		1348	41.35		333
	1788	1.26		628	15	1516	1.69	1.6	579
	1793	1.37		640		1465	1.76		911
	1681	1.29		1597		1605	1.66		278
11	1726	11.09	11.2	229		1618	1.57		263
	1803	10.75		93		1660	1.53		187
	1649	11.24		424	15	1177	9.13	7	1288
	1555	11.52		947		1228	8.58		1125
	1590	11.48		793		1312	9		712
12	1547	1.57	1.5	569		1388	8.53		489
	1629	1.5		272		1431	8.13		306
	1659	1.43		223		1468	7.51		225
	1682	1.34		162		1542	7.18		130
	1467	1.71		1273	16	1544	1.94	1.9	812
12	1335	11.84	10.6	1011		1647	1.77		407
	1390	11.07		630		1785	1.9		113
	1507	9.91		223		1770	1.95		119
	1616	9.02		82		1718	2.08		152
	1447	11.06		373					

Mix #	T (K)	P (atm)	P_{avg}	τ_{ign} (μs)
16	1457	9.14	8.8	508
	1633	7.16		126
	1557	7.81		240
	1358	10.05		1233
	1425	9.95		756
16	1471	14.12	14.2	359
	1506	13.51		254
	1533	12.75		181
	1414	15.1		540
	1338	15.34		959
17	1752	2.28	3.1	77
	1585	3.01		309
	1426	3.58		1147
	1514	3.45		589
17	1300	8.43	7.1	1713
	1441	7.26		499
	1520	6.92		306
	1556	6.66		251
	1596	6.35		191

VITA

Name: John M. Pemelton

Address: Department of Mechanical Engineering
3123 TAMU,
College Station, TX 77843

Email Address: jmpemelton@neo.tamu.com

Education: B.S., Mechanical Engineering, The University of Texas-Pan American, 2004

Experience: The University of TX-Pan American, Edinburg, TX, Fall 2004
Teacher Assistant (TA) for Heat Transfer in Mechanical Engineering Department

The Boeing Company, Everett, WA, 2005 - 2009
Systems Engineer in the 787-8 Fuel Systems, Fuel Quantity Indicating System (FQIS)

Texas A&M University, College Station, TX, 2009 – present
Graduate Assistant Researcher (GAR), Mechanical Engineering Department
Advisor: Dr. Eric L. Petersen.